Optimisation of carbon fibre reinforced polymer composites with a thin embedded polyurethane film

OPTIMISATION OF CARBON FIBRE REINFORCED POLYMER COMPOSITES WITH A THIN EMBEDDED POLYURETHANE FILM

Evanthia J. Pappa[1], Edward D. McCarthy[1] and Conchur O Brádaigh[1]

[1] The University of Edinburgh, School of Engineering, Institute for Materials and Processes, Edinburgh EH9 3FB, UK, e.pappa@ed.ac.uk

Keywords: CFRP, interleaves, toughness, out-of-autoclave, Mode I

ABSTRACT

The aim of this work is a preliminary study of interleaved hybrid polymer composites used for impact energy absorption. The interlaminar properties of optimised pre-impregnated carbon fibre reinforced polymer (CFRP) hybrid laminated composites, containing thermoplastic polyurethane (PU) interleaves, have been measured. Two common manufacturing methods have been used to manufacture the laminates; vacuum bag consolidation (VB) and hot press consolidation (HP). The interlaminar fracture toughness (Mode I) of the optimised laminates was twice that of the reference laminate for both VB and HP, and almost 10% higher when changing the manufacturing process from VB to HP. The results indicated good bonding between the thermoplastic interleave and the epoxy. The adhesion between the CFRP epoxy and the PU film has a significant effect on the crack propagation behaviour of the structure, e.g., fibre bridging is reduced, and there is good adhesion. To study this adhesion, scanning electron microscopy (SEM) was used to observe the interface between the two phases. The preliminary quasi-static tests show that there is no significant reduction of the mechanical properties of the optimised PU laminates. For this reason, thermoplastic materials are frequently used for absorption of impact energy to improve laminate damage tolerance.

1 INTRODUCTION

Fibre reinforced polymer (FRP) composite materials are being used in increasing volumes in the aerospace industry, e.g., Boeing Dreamliner, Airbus A350; more than 50% by weight of these aircraft are made of composite materials. Composite materials are used in both primary and secondary structural parts, for example, the main wing and the fuselage of these aircraft are manufactured in carbon fibre reinforced polymers (CFRPs) [1-2, 5-6,]. Their high specific strength and stiffness make them lighter than metallic parts for the same load duty. Laminated composites are the most frequent composite materials that are used in applications like aerospace engineering and wind energy. This is because they increase the flexibility of the design as ply fibre directions and layup sequences can be customised, they have greater corrosion and higher fatigue resistance than metal alloys [1-4].The fibre plies can be arranged in different orientations to provide in- plane or out-of-plane properties. Fibrous materials can be either unidirectional, woven, or braided to reinforce the polymeric matrix.

Pre- impregnated tapes (prepregs) are the most common materials that are used in the fabrication of such high performance components. There are two main manufacturing processes to produce a component from composite prepreg: autoclave and out-of-autoclave. Autoclave processing is robust; the component is placed in a sealed vacuum bag inside a heated pressure vessel. The applied pressure and the controlled temperature almost perfectly consolidates the prepreg and shapes it to a strong solid component. However, autoclave processing is a fairly expensive process to deploy, especially for large structures as it is time consuming and very energy inefficient. Therefore, out-of-autoclave (OoA) processes are used, in this paper, we used vacuum bag only (VBO) and hot press (HP) consolidation processes. However, for out-of-autoclave techniques, while there is a significant reduce in the operating costs, void content tends to be higher. To produce a void-free component, high pressure and good consolidation is necessary, especially for thick parts. Therefore, researchers are currently trying to tackle the high porosity levels in out-of-autoclave processes for high quality parts [3]. Therefore, hot pressing is an alternative manufacturing technique that is cost-effective and produces high quality parts. To use this technique effectively to produce a high quality part, it is necessary to equalize the

applied pressure throughout the enclosed mould, to ensure homogeneous consolidation and minimal dimensional deviation. Another important objective in manufacturing high quality components is to maintain uniform distribution of both resin and fibres and to maintain high, evenly distributed fibre volume fractions throughout the component. Therefore, laminate quality tests are of high importance.

Non-destructive testing methods have been successfully applied to inspect composite materials in detail. Those methods include ultrasound, X-ray tomography, thermography and digital image correlation. These are used to inspect composite laminates for accidental low velocity impact during manufacture or in-service. Undetected damage on a composite structure can reduce the mechanical properties and lead to severe damage or complete failure. Thus, both industry and academia are seeking to tackle this effect by introducing nanoparticles, interleaves, veils etc. [5-9] to improve the interlaminar toughness and impact properties. Interleaving can improve both the impact resistance and the interlaminar toughness, but can potentially adversely impact mechanical properties if not properly implemented. Poor adhesion of interleaves to laminae can easily lead to delamination and rapid crack propagation [9-12, 27]. This study addresses this issue, and investigates the interleave-CFRP adhesion.

To benchmark the delamination and crack propagation in a laminate composite it is important to measure its interlaminar fracture toughness and flexural properties. Interfacial interaction between the fibres and the epoxy as well as the composite's homogeneity are important factors for investigating fracture properties. One basic mode of delamination is mode I, where the delamination of unidirectional laminates (UD) follows a straight path along the interface in which the crack initiation has started. Fibre bridging occurs along this interfacial opening during peel tension, and is a form of residual resistance of the interface to crack propagation [8-9]. Studies in increasing interlaminar fracture toughness have employed carbon nanotubes (CNT) sheets and nanoparticles [12-14, 18, 19,], steel fibres [12], nanofibrous veils and interleaves [10, 16-20, 25], etc. In most cases, Mode I and Mode II toughness have been reported to increase considerably.

The double cantilever test (DCB) is used to determine interlaminar toughness specifically, it measures the critical interlaminar energy release rate G_{IC}. According to the standard ASTM D5528, this test determines the apparent interlaminar shear strength, which has a strong dependence on the geometry of the specimen. The delamination is a consequence of interlaminar normal stresses (peeling) rather than interlaminar shear stress (Mode II fracture). The current work presents a preliminary study on the optimisation of CFRP prepregs with an embedded thin polyurethane film. As stated before, thermoplastic interleaves are advantageous because of their high toughness [16-20]. We present an investigation of the adhesion properties for a thin film of thermoplastic interleave embedded in CFRP prepregs, targeted at optimisation of impact energy absorption.

2 MATERIALS AND PROCESSES

Initial trials were undertaken using 12 commercially available thermoplastic interleaves. These trials allowed for down selection of the most effective interleave material for applications in impact energy reduction. The following materials were used for the fabrication of the panels: pre-impregnated T700 carbon fibers (Toray) combined with a VTC401 epoxy, supplied by SHD Composite Materials Ltd., and 25μm thermoplastic polyurethane film, supplied by Schweitzer-Mauduit International (SWM) Ltd. In both cases, a standard lay-up process was used to manufacture the laminates. A stage-wise de-bulking process was implemented to achieve better consolidation. As previously mentioned, two out-of-autoclave consolidation options were used for this study, vacuum bag (VB) and hot press (HP), to produce the laminates. According to the supplier's instructions, the curing process should result in a glass transition temperature for the epoxy of ca. 118˚C. To maintain the quality of the laminates, the temperature was recorded throughout the curing process and final laminate densities were measured using Archimedes' test and volume fraction/void data, according to ISO 7822. Additionally, all laminates were scanned using an ultrasound system (Dolphicam) and optical characterisation of the through-thickness surface of various areas of the laminate to verify manufacturing quality. In all cases, a consistent laminate thickness of ca. 4 mm was achieved (See Table 1).

From the cured panels, rectangular specimens were cut with a diamond tip disk saw according to the standards for each test; ASTM D5528, ASTM D7264 and ISO 14130 for the double cantilever

beam (DCB) tests, the flexure tests and the short beam interlaminar shear strength, respectively. To determine delamination growth and bending displacement of DCB specimens in real time, a video gauge extensometer was used, supplied by Imetrum Ltd. The video extensometer provides a point-to-point precision measurement using a video gauge and identifying deflections across the region of interest. For both the DCB and flexural tests, an Instron 3360 machine was used, while for the ILSS tests a Zwick 3-97 was used. Scanning electron microscopy (SEM) images were taken to indicate the differences in adhesion properties between the laminates as a function of the manufacturing process after the DCB test.

3 RESULTS

3.1 Double Cantilever Beam (DCB)

The properties as derived from the DCB tests are shown in Table 1 below. The cases as described are vacuum-bagged reference laminate (VBREF), vacuum-bag laminate optimized with the PU interleave in the middle plane (VBPU), hot-pressed reference laminate (HPREF), and hot-pressed laminates optimized with the PU interleave in the mid- plane of the laminate (HPPU).

Cases	Thickness, h± 0.05 (mm)	Delamination length, α ± 0.05 (mm)	Mode I, G_{IC} (kJ/m^2)
VBREF	4.45	59.17	0.98 ± 0.12
VBPU	4.59	59.38	2.40 ± 0.33
HPREF	4.09	65.06	1.04 ± 0.25
HPPU	3.97	63.97	2.83 ± 0.79

Table 1: Mode I Test results for all laminates.

For the calculation of the mode I interlaminar fracture toughness, G_{IC}, load cell compliance was into account and the following expression was used:

$$G_{IC} = 3P\delta / 2b(\alpha+|\Delta|) \quad (1)$$

where P is the applied load, δ is the displacement, b is the width of the specimen, α is the delamination growth and Δ is the experimental compliance as a function of the load point displacement and the applied load.

Representative DCB load versus displacement curves for the four laminate types are shown in Fig. 1. The curves of all cases show an elastic region until the crack propagates and leads to interface separation as shown in the plots (Figure 1). The first peak on the curve is indicative of the crack initiation at the entry point of the crack. At this particular point, the crack stops growing momentarily, until there is sufficient strain energy to propagate the crack to the next point in the midplane; hence, the plot shows loads increasing and decreasing in a repetitive manner. The fact that the two interleaves show markedly higher loads throughout the interface separation phase indicates that the interleaves have a positive effect on the fracture toughness. Specifically, the Mode I critical fracture toughness, G_{IC}, is ca. twice as high when the PU interleave is introduced in the structure. Moreover, there is an increase in G_{IC} for HPPU of almost 6% compared with that of HPREF.

In all the cases, the critical strain rate increased in a range of delamination length, a, 55-65mm. Typical brittle behavior of crack propagation for thermoset Mode I specimens was observed almost in all cases for the reference samples. In the cases of VBREF and VBPU, this step-wise pattern that is observed in Fig. 1, is more intense than what might be caused by void coalescence in the specimens. Each void is a local load concentration area before it gathers enough energy to propagate a crack. Thus every step in the plot can be related to a local energy release rate. When using the hot press, brittle behavior is still present but barely noticeable. Conversely, for the plots that show crack propagation of the HPPU, the curves are much smoother as the void content is considerably smaller. Fibre bridging is a significant phenomenon when interpreting fracture toughness, as it represents the quality of the interface between the fibres and the matrix, i.e., extensive fibre bridging indicates a strong interface

and vice versa.

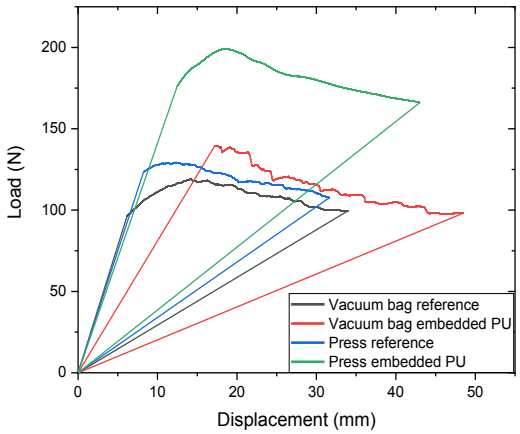

Figure 1: Load vs displacement plot for all the cases, a) VBREF (black line), b) VBPU (red line), c) HPREF (blue line) and d) HPPU (green line).

In Fig. 2, the fibre bridging effect can been seen to some extent for all the cases. However, the introduction of the interleave has almost totally eliminated the fibre bridging effect, especially for the hot press case (Fig. 2d). In fact, as the crack propagates from the insert region to the interleave region, it splits the film itself and not the interface between the epoxy and the film (i.e., there is cohesive rather than adhesive failure). A reason for this may be that during loading of the hot-pressed interleave sample (HPPU), more energy is required to separate the interface between the epoxy and the PU, as the interfacial bond is strong. The surfaces of the debonded HPPU specimens were smooth and showed relatively few fibre fragments (Fig. 2.d). Evidence of this typical thermoplastic behaviour is provided by a set of river lines [28] that occur once the crack has propagated through the HPPU specimen, and which indicate matrix shearing that can been seen in Figure 3b.

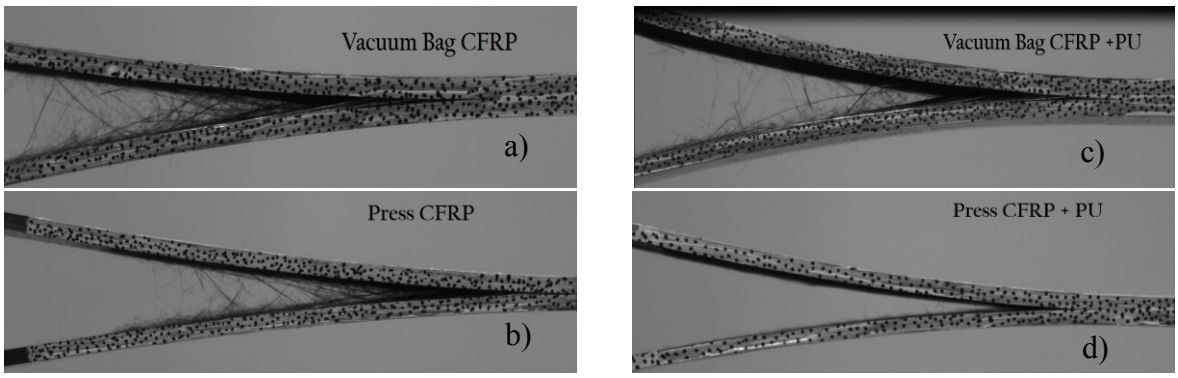

Figure 2: Fibre bridging effect for the specimens a) VBREF, b) HPREF, c) VBPU and d) HPPU.

By contrast, for the reference thermoset materials, the matrix resin generates a rougher surface during the peeling as the crack travels from the insert to the bonded specimen. The crack jumps abnormally because of the brittle nature of the epoxy and results in a rougher surface and the formation of long matrix filaments. Another significant observation is that the manufacturing process and the interleave both have an effect on Mode I behaviour. Poor consolidation can leave voids or air gaps causing the fibre-matrix interfacial adhesion to be poor, and thus, the effect of fibre bridging is higher (Fig 2.a & Fig 2.b), as voids are potentially local stress concentration areas. In the next section, Scanning Electron Microscopy (SEM) images indicate the differences between the fracture surfaces.

3.2 Scanning Electron Microscopy (SEM)

To obtain the SEM images after fracture, a Jeol JSM-IT100 InTouchScope was used. In Figs. 3 and Fig. 4, the morphology of the specimens after the DCB test can been seen. For the reference CFRP prepreg material, (Fig. 3a and Fig. 4a) the epoxy is smooth and featureless indicating an entirely brittle fracture, as would be expected for a homogeneous thermoset polymer. The fracture morphology is similar for both manufacturing processes. The carbon fibres peel off from the epoxy, leaving behind epoxy, which has broken into small smooth filaments.

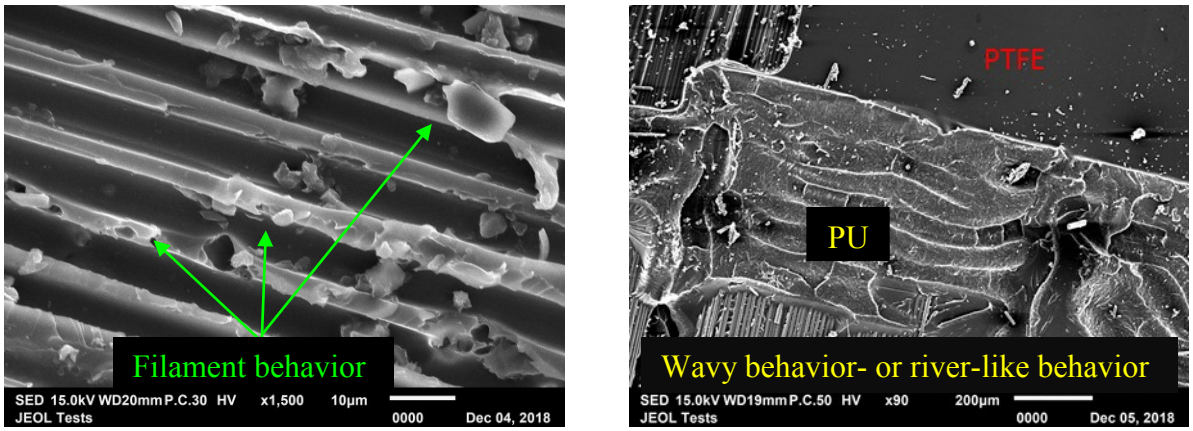

Figure 3: SEM images representing the fracture behaviour in the midplane after the DCB test of the a) VBREF and b) VBPU.

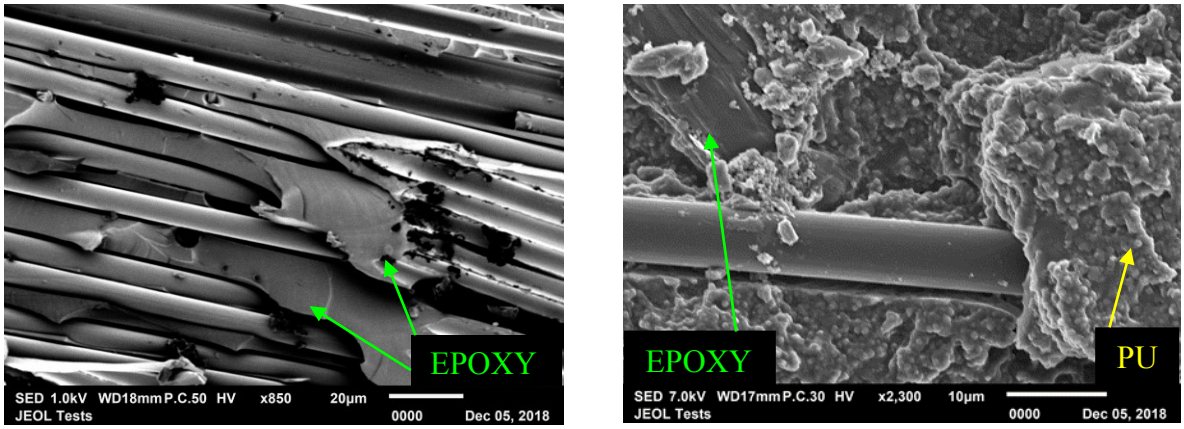

Figure 4: SEM images representing the adhesion behavior in the midplane after the DCB test of the a) HPREF and b) HPPU.

By contrast, when introducing a thermoplastic interleave like PU, a phenomenon known as reaction-induced phase separation takes place during the epoxy curing process [26]. During fracture, it appears that the thermoplastic particles of the interleave are plastically deformed and are drawn into peaks in the direction of crack growth, (Fig. 3.b), which produces wavy or river-like behaviour. That indicates that the film can maintain a strong interfacial bond during fracture, hence enhancing Mode I fracture toughness. Moreover, for the hot pressed manufactured specimens, (Fig. 4.b), there is a clearly visible interfacial bond between the epoxy and the PU; therefore, it is more difficult for the fibres to be peeled away. The latter is a well-established property of thermoplastic materials, as they have the ability to shear to a much greater extent than thermosets via plastic deformation and thus bear higher levels of strain energy.

3.3 Flexural testing

The transverse flexure properties of the hot press specimens were determined using a four- point bend test in accordance with the ASTM D7264. The span-to-thickness ratio was 32:1 and a minimum of 6 tests were conducted for each case. The loading rate was 1mm/min with a load cell of 10kN. When the load is applied, the test specimen deflects such that the underside of the specimen is under tension and the upper side will be subjected to compression forces. For sufficiently thin specimens, the effect of shear can be neglected; therefore, bending failure may be caused by either tensile or compressive stresses. For this study, the interface between the matrix and the interleave is of high importance; therefore, transverse flexure properties, which are dominated by the matrix and the interface rather than the fibre properties, were carried out. The fibres were oriented perpendicular to the test axis, and the interleave was placed in the midplane of the specimen. Table 2 presents the properties determined from this test:

Cases	Thickness, h ± 0.05 (mm)	Transverse Flexural Young's Modulus, M_f (GPa)	Transverse Flexural strength, σ_f (MPa)
HPREF	4.09	8.57 ±1.02	84.12
HPPU	3.97	8.62 ±0.32	75.85

Table 2: Transverse flexural properties.

The maximum flexural stress and strain can be calculated from the load-displacement curve using the following equations:

$$\sigma_f = 3Pl/4bh^2 \quad (2)$$

$$\varepsilon_f = 4.36\delta h/l^2 \quad (3)$$

where, P is the applied load, l is the length of the span, b is the width of the specimen, h is the thickness of the specimen, and δ is the middle span thickness.

Figure. 5 represents the stress-strain curves from the two cases studies, HPREF, and HPPU. Both cases follow the same trend, with almost completely elastic behaviour followed by a single, sudden failure. Tensile failure was observed for all specimens, i.e., they failed suddenly at the centre of the unsupported span of the specimen.

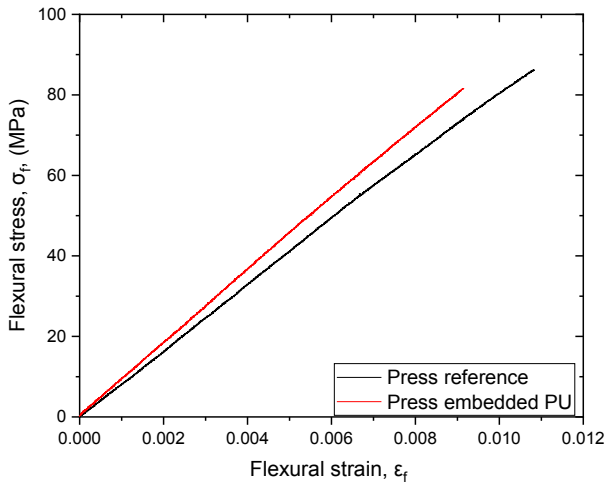

Figure 5: Transverse stress-strain curve for the HPREF (black line) and HPPU (red line).

3.4 ILSS Analysis

The short beam shear test is a three-point flexure test with a constant crosshead displacement rate and a span-to-thickness ratio of 5:1. The tests were carried out based on ISO 14130 with a support

span between 6.5mm and 6.7mm, depending on specimen thickness, and a loading rate of 1mm/min. The load was applied parallel to the direction of the fibres. In Figure 6 below, the interlaminar shear strength of the VB specimens are shown. To calculate their interlaminar shear strengths (ILSS), the following equation was used:

$$\tau_{max} = 3P_{max} / 4bh \quad (4)$$

where P_{max} is the maximum load, b is the width, and h is the thickness of the specimen.

Representative plots of force vs displacement for the VB ILLS tests are shown in Fig. 6. The ILSS test involves highly complex stress states, which are a combination of local contact stresses, as well as flexural and interlaminar shear stresses. Therefore, to obtain the interlaminar shear strength from a short beam test, the peak test load is used, with resulting values shown in Table 3.

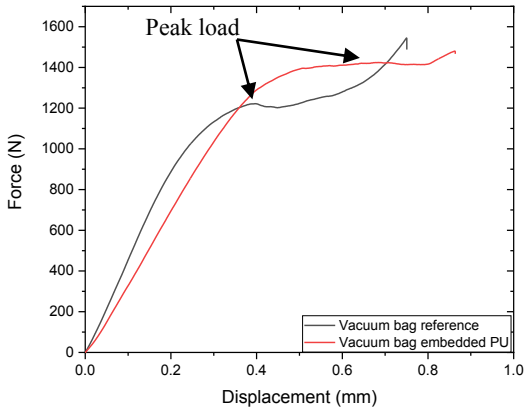

Figure 6: Short beam load versus displacement curve for a) VBREF (black line) and b) VBPU (red line).

The ILLS test curve shows a typical elastic region in the beginning (pseudo-linear section) and then it deforms plastically, until multiple shear locations were observed due to interlaminar shear failure in the specimen. The plateau of plastic deformation is observed in all the cases, and after that a sudden increase in loading which is a result of span resistance. Lastly, it is quite difficult to obtain a valid failure as local compression loading, crushing or flexural failure can occur; thus, peak loads are consider as more valid. From the analysis obtained, a slight decrease in the interlaminar shear strength is observed when introducing a PU interleave in the composite.

Cases	Thickness, h ± 0.05 (mm)	Interlaminar shear strength, τ_{max} (MPa)
VBREF	2.23	72.3 ±2.79
VBPU	2.26	71.5 ±1.28

Table 3: Interlaminar shear strength (ILSS) properties (No. of specimens = 6 each).

4 CONCLUSIONS

A study on the interfacial properties of a prepreg CFRP composite material with an embedded PU interleaf has been presented in this paper. Out-of-autoclave manufacturing processes were used for the fabrication of unidirectional laminates. The two manufacturing processes showed different behavior for the interlaminar shear toughness as the void content has an effect on the toughness and the adhesion properties of the laminates. In fact, there is an increase in toughness of almost 6% for reference press specimens compared with reference vacuum-bagged specimens. However, with the introduction of a thin polyurethane film to press-moulded laminates, the mode I critical fracture toughness was almost double that of the reference CFRP material. This is an indication that the adhesion between the epoxy and the thermoplastic film was excellent. SEM images showed that there

was good adhesion between the epoxy and PU films, especially for the press specimens. Transverse four-point bending tests were also carried out to determine the effect of the matrix and interface on flexural properties. ILLS tests were also performed, and in both tests there is no significant degradation of the CFRP mechanical properties when using the PU film. In conclusion, the use of PU films, especially in a press process, is shown to significantly increase Mode I toughness, so that it can be considered as a promising means of reducing impact damage tolerance (strongly linked to toughness) without significantly compromising other laminate properties.

ACKNOWLEDGEMENTS

The authors would like to acknowledge the Institution of Mechanical Engineers (IMechE) and the University of Edinburgh, especially the School of Engineering, for the financial support. Moreover, acknowledgements are also given to Composites Testing Laboratory (CTL), Galway Ireland, for the instrumental support.

REFERENCES

[1] N.H. Nash, T.M. Young, P.T. McGrail, W.F. Stanley "Inclusion of a thermoplastic phase to improve impact and post-impact performance of carbon fibre reinforced thermosetting composites- A review". *Materials & Design*, 85, 2015, pp. 582-597.

[2] M. Yasaee, I.P. Bond, R.S. Trask, E.S. Greenhalgh "Damage control using discrete thermoplastic film inserts", *Composites, Part A*, 43, 2012 pp. 978-989.

[3] S.E. Boyd, T.A. Bogetti, J.M. Staniszewski, B.D. Lawrence, M.S. Walter "Enhanced delamination resistance of thick-section glass-epoxy composite laminates using compliant thermoplastic polyurethane interlayers", *Composite Structures*, 189, 2018, pp. 184-191.

[4] H. Kishi, M. Kuwata, S. Matsuda, T. Asami, A. Murakami "Damping properties of thermoplastic- elastomer interleaved carbon fiber- reinforced epoxy composites", *Composites Science and Technology*, 64, 2004, pp. 2517-2523.

[5] C. Sonnenfeld, H. Mendil-Jakani, R. Agogue, Philippe Nunez, P. Beauchene "Thermoplastic/thermoset multilayer composites: A way to improve the impact damage tolerance of thermosetting resin matric composites", *Composite Structures*, 171, 2017, pp. 298-305.

[6] P. E. Irving and C. Soutis, *Manufacturing processes for composite materials and components for aerospace applications*, Polymer composites in the Aerospace Industry, Vol. 1, Woodhead Publishing, UK, 2014

[7] S. Rana and R. Fangueiro, *Advanced Composite Materials for aerospace Engineering*, Vol. 1, Woodhead Publishing, Portugal, 2016

[8] T. Centea, L. K. Grunenfelder, S. R. Nutt, A review of out-of-autoclave prepregs- Material properties, process phenomena, and manufacturing considerations, *Composites Part A: Applied Science and Manufacturing*, 70, 2015, pp. 132-154.

[9] G. Frossard, J. Cugnoni, T. Gműr, J. Botsis, Mode I Interlaminar fracture of carbon epoxy laminates: Effects of ply thickness, *Composites Part A: Applied Science and Manufacturing*, 91, 2016, pp. 1-8.

[10] D. Quan, J. L. Urdaniz, A. Ivanković, Enhancing mode-I and mode-II fracture toughness of epoxy and carbon fibre reinforced epoxy composites using multi-walled carbon nanotubes, *Materials & Design*, 143, 2018, pp. 81-92.

[11] M. Yasaee, I. P. Bond, R. S. Trask, E. S. Greenhalgh, Mode I interfacial toughening through discontinuous interleaves for damage suppression and control, *Composites Part A: Applied Science and Manufacturing*, 43, 2012, pp. 198-207.

[12] G. W. Beckermann, K. L. Pickering, Mode I and Mode II interlaminar fracture toughness of composite laminates interleaved with electrospun nanofibre veils, *Composites Part A: Applied Science and Manufacturing*, 72, 2015, pp. 11-21.

[13] V. Eskizeybek, A. Yar, A. Avci, CNT-PAN hybrid nanofibrous mat interleaved carbon/epoxy laminates with improved Mode I interlaminar fracture toughness, *Composites Science and Manufacturing*, 157, 2018, pp. 30-39.
[14] R. J. Cano, B.W. Grimsley, J. H. Kang, J. G. Ratcliffe, E. J. Siochi, Properties of Multifunctional Hybrid Carbon Nanotube/Carbon Fiber Polymer Matrix Composites, *TechConnect Briefs*, 1, 2016, pp. 221-224
[15] D. Quan, S. Flynn, M. Artuso, N. Murphy, C. Rouge, A. Ivankovic, Interlaminar fracture toughness of CFRPs interleaved with stainless steel fibres, *Composite Stuctures*, 210, 2019, pp. 49-56.
[16] N. Zheng, Y. Huang, H. Liu, J. Gao, Y. Mai, Improvement of interlaminar fracture toughness in carbon fiber/epoxy composites with carbon nanotubes/polysulfone interleaves, *Composites Science and Technology*, 140, 2017, pp. 8-15.
[17] B. Beylergil, M. Tanoğlu, E. Aktaş, Enhancement of interlaminar fracture toughness of carbon fiber‐epoxy composites using polyamide‐6,6 electrospun nanofibers, *Journal of Applied Polymer Science*, 134, 2017, 45244, (doi: 10.1002/app.45244).
[18] C. Hunt, J. Kratz, I. Partridge, Cure path dependency of mode I fracture toughness in thermoplastic particle interleaf toughened prepreg laminates, *Composites Part A: Applied Science and Manufacturing*, 87, 2016, pp. 109-114.
[19] M. Fotouhi, C. Fragassa, S. Fotouhi, H. Saghafi, G. Minak, Damage Characterization of Nano-Interleaved CFRP under Static and Fatigue Loading, *Fiber Reinforced Inorganic-based Composite Systems for Structural Applications,* 7, 2019, 13 (https://doi.org/10.3390/fib7020013).
[20] H. Saghafi, S. R. Ghaffarian, T. M. Brugo, G. Minak, A. Zucchelli, H. A. Saghafi, The effect of nanofibrous membrane thickness on fracture behaviour of modified composite laminates – A numerical and experimental study, *Composites Part B: Engineering*, 101, 2016, pp. 116-123.
[21] T. Brugo, G. Minak, A. Zucchelli, X. T. Yan, J. Belcari, H. Saghafi, R. Palazzetti, Study on Mode I fatigue behaviour of Nylon 6,6 nanoreinforced CFRP laminates, *Composite Structures*, 8, 2017, pp 1-8.
[22] L. Liu, L. Shen, Y. Zhou, Improving the interlaminar fracture toughness of carbon/epoxy laminates by directly incorporating with porous carbon nanotube buckypaper. *Journal of Reinforced Plastics and Composites*, 35, 2016, pp. 165-176.
[23] F. Narducci, K. Y. Lee, S. T. Pinho, Interface micro-texturing for interlaminar toughness tailoring: a film-casting technique, *Composites Science and Technology*, 156, 2018, pp. 203-214.
[24] J. J. Stahl, A. E. Bogdanovich, P. D. Bradford, Carbon nanotube shear-pressed sheet interleaves for Mode I interlaminar fracture toughness enhancement, *Composites Part A: Applied Science and Manufacturing*, 80, 2016, pp. 127-137.
[25] V. Damodaran, A. G. Castellanos, M. Milostan, P. Prabhakar, Improving the Mode-II interlaminar fracture toughness of polymeric matrix composites through additive manufacturing, *Materials & Design*, 157, 2018, pp. 60-73.
[26] R. J. J. Williams, B. A. Rozenberg, J. P. Pascault, Reaction-induced phase separation in modified thermosetting polymers, *Advances in Polymer Science*, 128, 2005, pp.95-156.
[27] E.D. McCarthy and C. Soutis, Determination of interfacial shear strength in continuous fibre composites by multi-fibre fragmentation: A review, *Composite part A: Applied Science and Manufacturing*, 118, 2019, pp. 281-292.
[28] E. S. Greenhalgh, *Failure analysis and Fractography of Polymer Composites*, Woodlead Publishing, 1, 2009, pp. 164-237.